

Fast Atom Bombardment Mass Spectra of the β -Blocker Nipradilol with Nitrate Ester Group–Tandem Mass Spectrometry (MS/MS) and B/E Constant Linked Scanning

Michiaki YONEDA,^a Kazuo TSUJIMOTO,^a Mamoru OHASHI,^{*a} Masami SHIRATSUCHI,^b Yasushi OHKAWA^b and Kimio ISA^c

Department of Applied Physics and Chemistry, University of Electro-Communications,^a Chofu-shi, Tokyo 182, Japan, Tokyo Research Laboratories Kowa Co., Ltd.,^b 2-17-43 Noguchi-cho, Higashimurayama-shi, Tokyo 189, Japan and Department of Chemistry, Faculty of Education, Fukui University,^c Fukui-shi 910, Japan. Received April 23, 1990

Fast atom bombardment (FAB) or liquid secondary ion mass spectra (LSIMS) of nipradilol and its analogues exhibit intense $[MH-45]^+$ ions corresponding to MH^+ ions of those hydrolysis products. Although FAB low energy collision-activated dissociation (CAD)-tandem mass spectrometry (MS/MS) using a triple-stage quadrupole-type instrument indicates that both ions are identical, the FAB(LSIMS) B/E constant linked scanning spectra of the ions are different from each other. To elucidate the reason for the two methods used for the same purpose giving different results, FAB high energy CAD-MS/MS was carried out using an EBE sector-type instrument. Comparison between the results of the B/E constant linked scanning and those of the high energy CAD-MS/MS indicated that the discrepancy is due to the poor resolution of precursor ions in the linked scanning at the B/E constant. It was also found that the high energy CAD-MS/MS spectra differed from the low energy CAD-MS/MS spectra owing to the difference in CAD energy between the two instruments. Decomposition products of nipradilol under FAB conditions were identified by high performance liquid chromatography and confirmed that the structures of the $[MH-45]^+$ ions were MH^+ of the hydrolysis products. The reaction products by fast atom bombardment under FAB conditions turned out to be the corresponding hydrolysis products which are different from those obtained by heating in glycerol.

Keywords nipradilol; β -blocker; FAB spectrum; B/E constant linked scanning; tandem mass spectrometry; MS/MS

Nipradilol,¹⁾ 3,4-dihydro-8-(2-hydroxy-3-isopropylamino)propoxy-3-nitroxy-2H-1-benzopyran (**1**), is a synthetic antihypertensive drug with β -blocking and vasodilating actions.²⁾ Nipradilol has both a nitrate ester group and an amino alcohol moiety, which is common to many β -blocking drugs such as propranolol and pindolol. In a previous paper, we reported that both electron impact (EI) and fast atom bombardment (FAB) or liquid secondary ion mass spectra (LSIMS) of **1** exhibit intense $[M-44]^+$ peaks at m/z 282.³⁾ The composition of the ion obtained in the EI mode is $[M-C_2H_4O]^+$ corresponding to the elimination of C_2H_4O from amino alcohol moiety, while that in the FAB (LSIMS) mode is $[MH-NO_2+H]^+$ corresponding to the hydrolysis or the ester exchange reaction product of the nitrate ester group. The structure of the $[M-44]^+$ ion on FAB (LSIMS) was confirmed to be identical with that of the MH^+ (protonated molecule) ion of the hydrolysis product (**8**) by FAB low energy collision-activated dissociation (CAD)-tandem mass spectrometry (MS/MS), using a triple-stage quadrupole mass spectrometer. However, the low energy CAD-MS/MS mainly gives the daughter ions produced by the cleavage of the amino alcohol moiety, but few ions associated with the cleavage of the skeleton part. We also attempted the linked scanning measurement at B/E constant to interpret the fragmentation process observed in the FAB (LSIMS) spectrum of **1**. At this stage, we expected that the B/E constant linked scan spectrum of $[M-44]^+$ ion of **1** should be identical with that of MH^+ ion of **8**, but it turned out that the spectra were different from each other. To account for this discrepancy, we measured FAB high energy CAD-MS/MS spectra using a sector EBE-type mass spectrometer, and solved the problem. This paper deals with the fragmentation pathways of **1** on the basis of the results obtained by B/E constant linked scanning and high energy CAD-MS/MS measurements.

Experimental

Materials Table I lists the compounds examined. Their origin was as

described previously.³⁾

Mass Spectrometry FAB mass spectra were obtained on a JEOL JMS-D300 mass spectrometer and LSIMS was performed on a Hitachi M-80B mass spectrometer. FAB high energy CAD-MS/MS was performed on a JEOL JMS-DX303 (EBE-type) mass spectrometer. The instruments were calibrated to standard mass values using glycerol-cesium iodide-sodium iodide.⁴⁾ The FAB guns (xenon atoms) were operated at 6 kV and the SIMS gun (xenon ions) at 8 kV. The ion accelerating voltages in these instruments were 3 kV. Glycerol was used as the matrix. High-resolution measurements were carried out on the JMS-D300 with a JMS-2000 mass data system using a mixture of polyethylene glycol (PEG) 200 and PEG 400 (1:1) as both the matrix and the standard. B/E constant linked scan experiments were performed on the M-80B with a Hitachi M-0101 mass data system. High energy CAD-MS/MS data were treated with a JEOL DA-5000 mass data system.

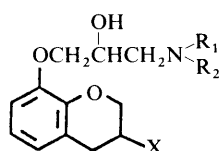
Decomposition of Nipradilol in Glycerol A small amount of nipradilol (about 0.1 mg) was directly mixed with glycerol (about 10 μ l), then applied on a FAB target and exposed to the FAB beam for 30 min. The mixture was eluted from the target with MeOH and injected into a high performance liquid chromatograph (HPLC). Nipradilol (10 mg) was dissolved in MeOH (0.1 ml) by heating and then mixed with glycerol (1 ml). The solution was heated at 100 °C for 3 h, then diluted with MeOH and injected into HPLC. HPLC was performed with a JASCO TRI ROTAR-III equipped with a UVDEC-100III detector. HPLC conditions were as follows: column, μ Bondapak- C_{18} (3.9 \times 300 mm); column temperature, 30 °C; mobile phase, H_2O -MeCN- CH_3COOH -10% (CH_3)₄NOH (500:150:5:1); flow rate, 1.5 ml/min; detection, UV 275 nm.

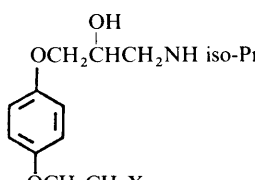
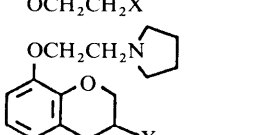
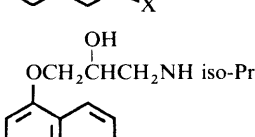
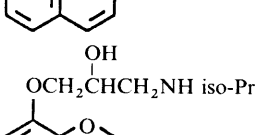
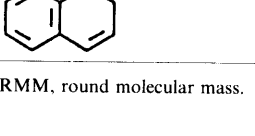
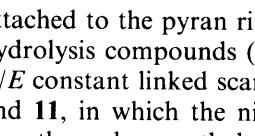
Results and Discussion

The FAB (LSIMS) spectra of **1**, **3**–**7** and **11** using glycerol as the matrix exhibit very intense MH^+ and $[MH-45]^+$ ($[M-44]^+$) ions, whereas those of hydrolysis products (**8**–**10** and **12**) show only MH^+ ions but no $[MH-45]^+$ ions. LSIMS spectra of **1** and **8** are shown in Fig. 1. Major ions of **1**–**15** are listed in Table II.

The B/E constant linked scan spectra of $[MH-45]^+$ and MH^+ ions clarified that $[MH-45]^+$ ion (P , m/z 282) of **1** gives $[P-30]^+$ ion (m/z 252), but this ion is not produced from the MH^+ ion (m/z 282) of **8**. Other daughter ions are almost identical in the two spectra (Fig. 2). Similar results were obtained between the linked scan spectra of other nitrate esters (**3**–**6**) in which the ester group is directly

TABLE I. Nipradilol and Its Analogues Investigated

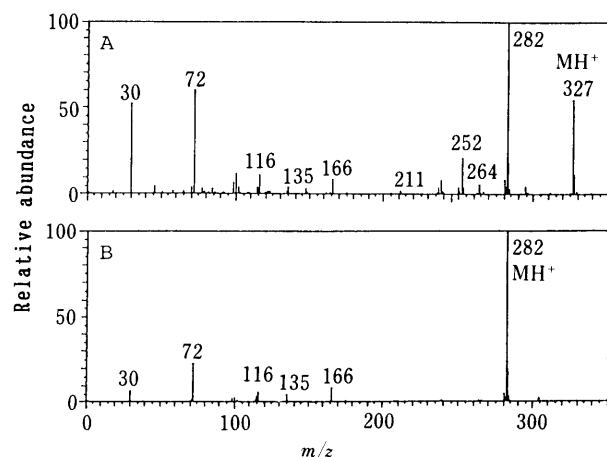
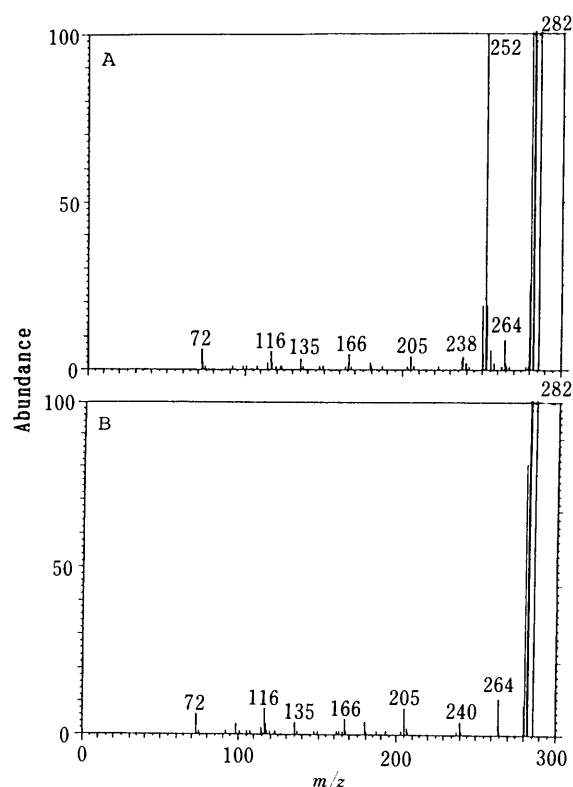
				
Compound	RMM	R ₁	R ₂	X
1	326	H	iso-Pr	ONO ₂
3	284	H	H	ONO ₂
4	312	H	Et	ONO ₂
5	340	H	<i>tert</i> -Bu	ONO ₂
6	340	Et	Et	ONO ₂
7	340	H	iso-Pr	CH ₂ ONO ₂
8	281	H	iso-Pr	OH
9	295	H	<i>tert</i> -Bu	OH
10	295	H	iso-Pr	CH ₂ OH

Structure	Compound	RMM	X
	11	314	ONO ₂
	12	269	OH
	13	308	ONO ₂
	14	263	OH
	2	259	
	15	263	

RMM, round molecular mass.

attached to the pyran ring and those of the corresponding hydrolysis compounds (**9** and **10**). On the other hand, the *B/E* constant linked scan spectra of $[\text{MH}-45]^+$ ions of **7** and **11**, in which the nitrate ester group is bound to the ring through a methylene group, are similar to those of MH^+ ions of the corresponding hydrolysis products **10** and **12**, respectively.

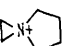
The results obtained from *B/E* constant linked scan spectra suggest that the structure of $[\text{MH}-45]^+$ ion of **1** is different from that of the MH^+ ion of **8**. The results from the low energy CAD-MS/MS, however, indicated that the two ions are identical as shown in the previous paper.³⁾ The phenomenon that the two methods used for the same purpose gave different results is remarkable. The *B/E* constant linked scan spectrum of MH^+ ion of **1** exhibits three intense peaks at m/z 281 ($[\text{MH}-46]^+$), m/z 252 ($[\text{MH}-75]^+$) and m/z 238 ($[\text{MH}-89]^+$). The spectra of MH^+ ions of **3–6** exhibit similar intense peaks. The

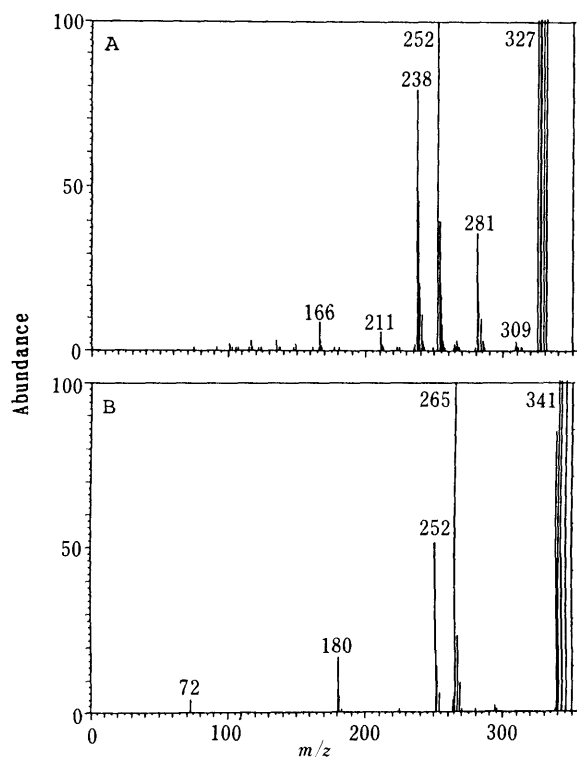
Fig. 1. LSIMS Spectra of (A) **1** and (B) **8**Fig. 2. FAB *B/E* Constant Linked Scan Spectra of (A) the $[\text{MH}-45]^+$ ion of **1** and (B) the MH^+ ion of **8** at m/z 282

intensities of $[\text{MH}-46]^+$ and $[\text{MH}-89]^+$ ions of these compounds are 40–60 and 70–100% against those of $[\text{MH}-75]^+$ ions, the most intense daughter ion in the spectrum, respectively. In contrast, *B/E* constant linked scan spectra of MH^+ ions of **7** and **11** exhibit intense $[\text{MH}-76]^+$ and $[\text{MH}-89]^+$ ions, but very weak $[\text{MH}-46]^+$ ions. These spectra of MH^+ ions indicate that the difference of the binding-type of the nitrate ester group to the ring is reflected in the intensity of $[\text{MH}-46]^+$ ion. As an explanation of the discrepancy mentioned above, we assumed that the *B/E* constant linked scan spectrum of $[\text{MH}-45]^+$ ion (m/z 282) of **1** overlapped that of $[\text{MH}-46]^+$ ion (m/z 281) because of the poor resolution of the precursor ion in the *B/E* constant linked scanning.⁵⁾ Thus, the spectrum of $[\text{MH}-45]^+$ ion of **1** differs from

TABLE II. Major Ions in LSIMS Mass Spectra of Nipradilol and Its Analogues

Compound	MH ⁺	[MH-45] ⁺	[MH-46] ⁺ a	[MH-63] ⁺ b	[MH-75] ⁺ c	[MH-89] ⁺ d	e	f	g
1	327 (55)	282 (100)	281 (6)	264 (8)	252 (21)	238 (23)	116 (11)	98 (6)	72 (60)
2	260 (100)	—	—	—	—	—	116 (8)	98 (2)	72 (18)
3	285 (100)	240 (65)	239 (4)	222 (9)	210 (14)	196 (8)	—	—	30 (10)
4	313 (93)	268 (100)	267 (7)	250 (17)	238 (49)	224 (19)	102 (69)	84 (92)	58 (83)
5	341 (79)	296 (94)	295 (6)	278 (8)	266 (27)	252 (8)	130 (17)	—	86 (100)
6	341 (26)	296 (63)	295 (5)	278 (3)	266 (12)	252 (6)	130 (3)	112 (8)	86 (100)
7	341 (24)	296 (18)	295 (1)	—	265 (4) ^{b)}	—	116 (14)	98 (9)	72 (100)
8	282 (100)	—	281 (2) ^{a)}	—	—	—	116 (5)	98 (3)	72 (21)
9	296 (100)	—	295 (3) ^{a)}	—	—	—	130 (6)	—	86 (62)
10	296 (100)	—	295 (3) ^{a)}	—	—	—	116 (13)	98 (8)	72 (74)
11	315 (44)	270 (21)	269 (1)	—	239 (8) ^{b)}	—	116 (23)	98 (5)	72 (100)
12	270 (100)	—	269 (3) ^{a)}	—	—	—	116 (11)	98 (4)	72 (100)
13	309 (65)	264 (44)	263 (6)	—	234 (14)	—	—	98 (43) ^{c)}	84 (100)
14	264 (100)	—	263 (6) ^{a)}	—	—	—	—	98 (68) ^{c)}	84 (98)
15	264 (100)	—	—	—	—	—	116 (9)	98 (8)	72 (36)

a) M⁺. b) [MH-76]⁺. c) . e, CH₂CHCH₂NHR₁R₂; f, CH₂=CH-CH=NR₁R₂; g, CH₂=NR₁R₂.

Fig. 3. FAB B/E Constant Linked Scan Spectra of the MH⁺ Ions of (A) 1 and (B) 7

that of MH⁺ ion of **8**, while the spectra of [MH-45]⁺ ions of **7** and **11** are similar to those of MH⁺ ions of **10** and **12**, respectively, because of the very weak intensities of [MH-46]⁺ ions of these compounds. Compound **4–6** gave results similar to that of **1**. The B/E constant linked scan spectra of the MH⁺ ions of **1** and **7** are shown in Fig. 3.

The complete separation of the precursor ion, [MH-45]⁺, from the [MH-46]⁺ ion is necessary to confirm the assumption described above. High energy CAD-MS/MS was, therefore, carried out using an EBE-type instrument (Fig. 4). The CAD-MS/MS of [MH-45]⁺, [MH-46]⁺ and [MH-47]⁺ ions (*m/z* 282, 281 and 280) of **1** were

compared with those of MH⁺, M⁺ and [M-1]⁺ ions (*m/z* 282, 281 and 280) of **8**, respectively, since [MH-46]⁺ and [MH-47]⁺ ions should influence the B/E constant linked scan spectrum of [MH-45]⁺ ion of **1**. The high energy CAD-MS/MS spectrum of [MH-45]⁺ ion (P) of **1** is almost identical to that of MH⁺ ion of **8**. The spectrum of [MH-46]⁺ ion of **1** is different from that of M⁺ of **8**, i.e. the [MH-46]⁺ ion (*m/z* 281) gives intense [P-30]⁺ ion (*m/z* 252), but this ion barely appears from M⁺ of **8** and the intensity of the daughter ion of **1** at *m/z* 238 is larger than that of **8**. The [MH-47]⁺ ion (*m/z* 280) of **1** also gives daughter ions at *m/z* 96, 187 and 250 more abundant than those from [M-1]⁺ ion of **8**. The comparison between the B/E constant linked scan spectra and the CAD-MS/MS spectra brings the conclusion that the B/E constant linked scan spectrum of the [MH-45]⁺ ion of **1** overlaps with those of [MH-46]⁺ and [MH-47]⁺ ions, and that the intense daughter ion peak at *m/z* 252 in the B/E constant linked scan spectrum of [MH-45]⁺ ion is actually produced from [MH-46]⁺ ion but not from [MH-45]⁺ ion. A real precursor ion of the ion at *m/z* 252 is [MH-46]⁺ ion (*m/z* 281), even though the intensity of the [MH-46]⁺ ion is only several percent of [MH-45]⁺ ion in the FAB (LSIMS) spectrum of **1**. Nevertheless, the ion at *m/z* 252 in the B/E constant linked scan spectrum of [MH-45]⁺ ion appeared as the most intense peak.

The [MH-45]⁺ ion is very intense in the FAB (LSIMS) spectrum, but [MH-45]⁺ ion (*m/z* 282) does not appear in the CAD-MS/MS spectrum of MH⁺ of **1**.³⁾ This indicates that the daughter ion cannot be derived unimolecularly from the MH⁺ ion in the gas phase, but is formed by protonation of the hydrolysis product produced from **1** on the target upon FAB. To confirm this conclusion, decomposition products of the sample bombarded with the xenon beam were examined by HPLC, i.e., **1** in glycerol was exposed to the FAB beam for 30 min, then eluted from the target and injected into HPLC. Peaks of **8** and **15** were observed on the chromatogram (Fig. 5). When a solution of **1** in glycerol was heated at 100 °C for 3 h, however only **15** but no **8** was detected as the decomposition product. This study certified

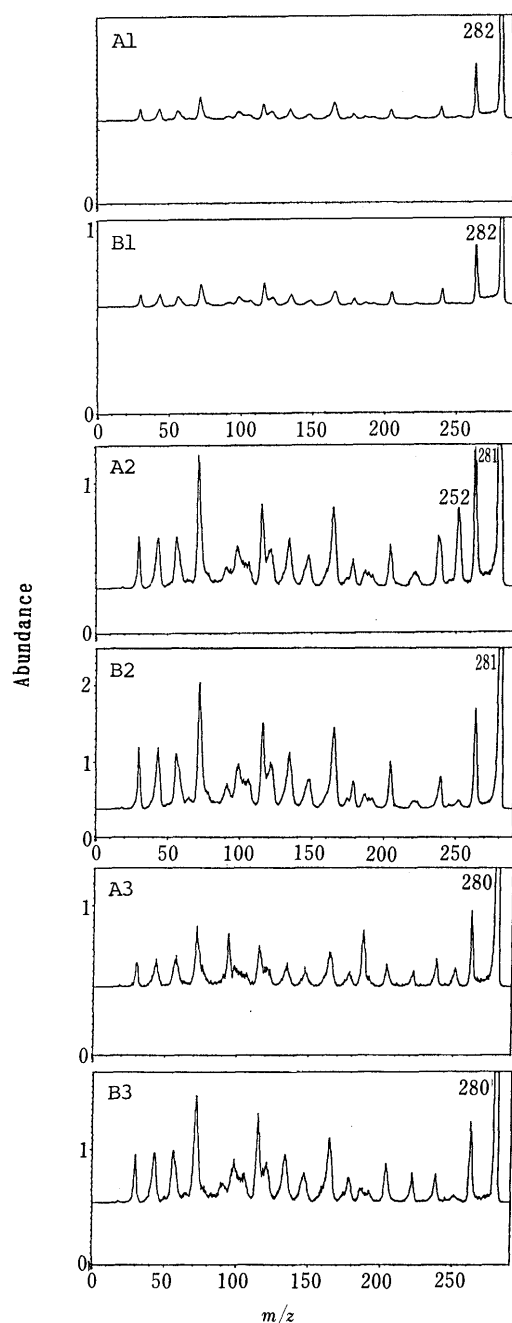


Fig. 4. FAB High Energy CAD-MS/MS Daughter Ion Spectra of the Ions of **1** and **8** at m/z 282, 281 and 280

A1, A2 and A3: $[MH-45]^+$, $[MH-46]^+$ and $[MH-47]^+$ ions of **1**. B1, B2 and B3: MH^+ , M^+ and $[M-1]^+$ ions of **8**.

that the conversion from **1** to **8** occurs on the target by bombarding with the xenon beam. Although many interfacial chemical reactions accompanying FABMS have been reported,⁶⁾ our finding is the first example that hydrolysis or ester exchange reactions take place under FAB conditions. Furthermore, the fact that the reactions under FAB conditions are different from those under heating must be very important from the viewpoint of reactions triggered by atom (ion) bombardment. We will discuss this point in detail elsewhere.

In the previous paper,³⁾ we reported the major fragments produced by cleavage of the amino alcohol moiety of **1** on the basis of the low energy CAD-MS/MS spectra. It is well

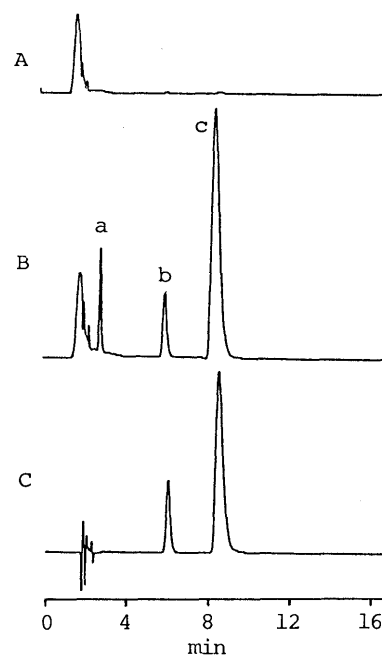


Fig. 5. HPLC of the Decomposition Products of **1**

A, glycerol matrix bombarded with xenon beam (FAB); B, reaction mixture of **1** after bombardment under FAB conditions; C, reaction mixture of **1** in glycerol after heating at 100 °C for 3 h; a, **8**; b, **15**; c, nipradilol.

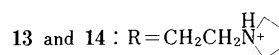
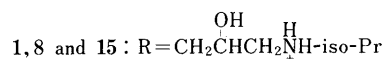
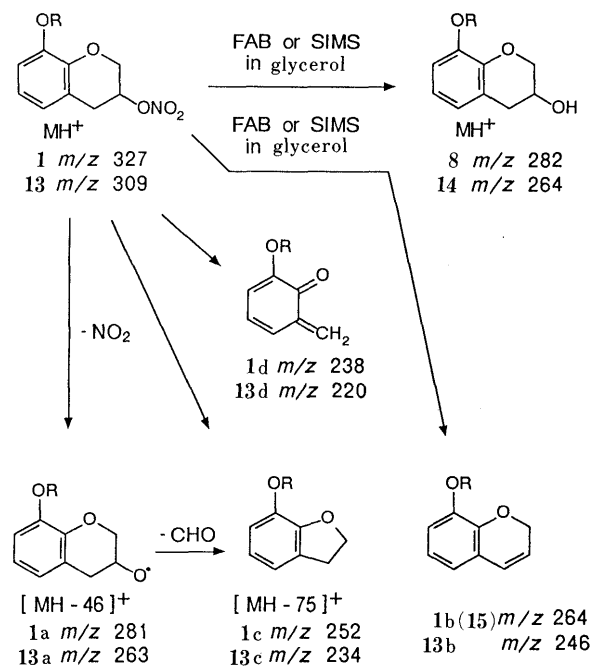


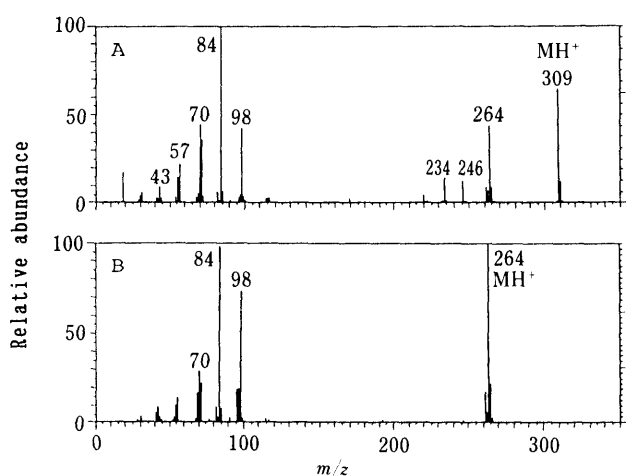
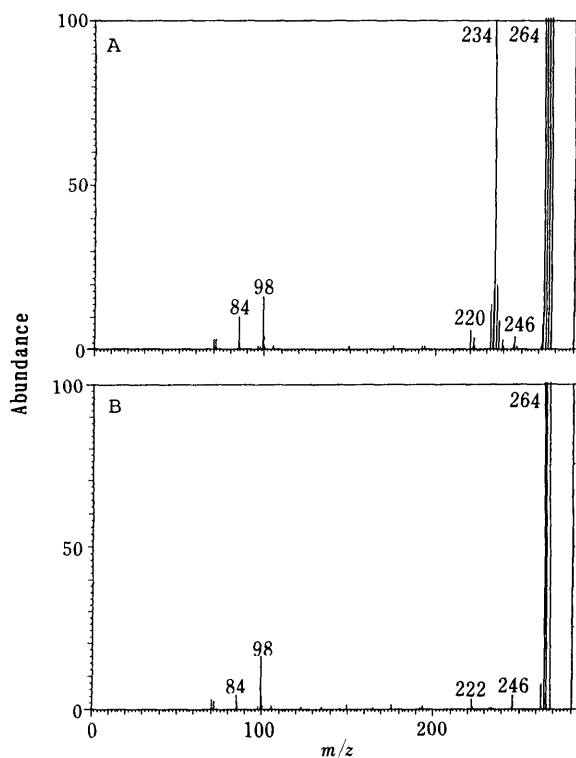
Chart 1

known that many charge remote fragmentations require keV collision activation (CA) and hardly arise from low eV CA.⁷⁾ Thus, the B/E constant linked scanning and the high energy CAD-MS/MS spectra exhibit the intense daughter ions produced by the cleavage of the skeleton part, although these ions are hardly apparent in the low energy CAD-

MS/MS spectra. Thus, it has now become possible to investigate the charge remote fragmentation⁸⁾ of the skeleton part on FAB (Chart 1). These techniques revealed that the major fragment ions from the MH^+ of **1** are **1a**, **1c** and **1d**. The ion **1a** is considered to be a radical cation produced by elimination of NO_2 radical, the ion **1c** is a ring

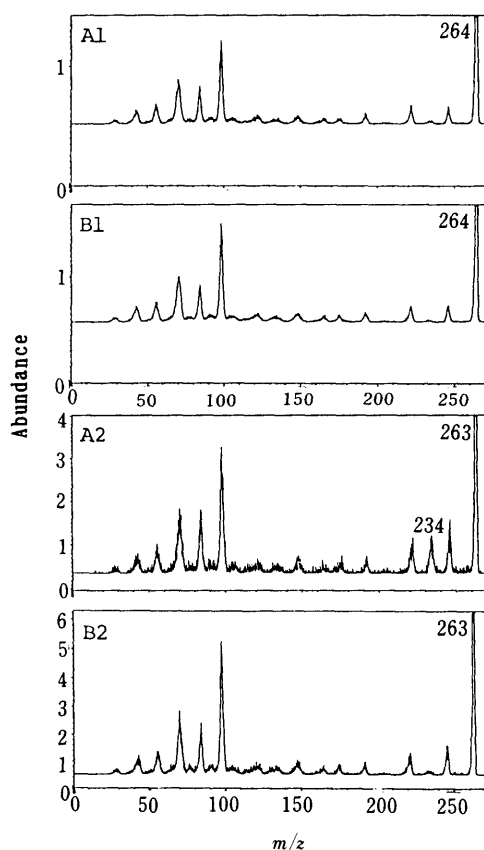
TABLE III. Accurate Mass Measurements of the Fragment Ions of **1**

Ion	Observed mass	Error (mmu)	Formula
$[MH-45]^+$	282.1700	-0.2	$C_{15}H_{24}NO_4$ $[MH-NO_2+H]$
1a	281.1610	-1.5	$C_{15}H_{23}NO_4$ $[MH-NO_2]$
1b	264.1614	1.5	$C_{15}H_{22}NO_3$ $[MH-HONO_2]$
1c	252.1624	2.5	$C_{14}H_{22}NO_3$ $[MH-CHONO_2]$
1d	238.1435	-0.5	$C_{13}H_{20}NO_3$ $[MH-CH_2CHONO_2]$

Fig. 6. LSIMS Spectra of (A) **13** and (B) **14**Fig. 7. FAB B/E Linked Scan Spectra of (A) the $[MH-45]^+$ Ion of **13** and (B) the MH^+ Ion of **14**

contraction product, and the ion **1d** is produced by the retro-Diels-Alder-type reaction. A similar fragmentation has been reported in EI spectra of 3-hydroxytetrahydropyran.⁹⁾ Neutral compounds **8** and **1b** (**15**) are produced from **1** on the target on FAB, and then respectively give the corresponding MH^+ ions in the mass spectra. The compositions of these ions were confirmed by high-resolution mass measurements (Table III).

To confirm the above conclusion, we examined the behavior of the pair of compounds **13** and **14**, as simpler models of **1** and **8**. FAB (LSIMS) spectrum of **13** exhibits the intense $[MH-45]^+$ ion (m/z 264) which corresponds to the MH^+ ion (m/z 264) of the hydrolysis product **14** (Fig. 6). The B/E constant linked scan spectrum of the $[MH-45]^+$ ion of **13** is, however, different from that of MH^+ of **14**, i.e. the $[MH-45]^+$ ion (P) of **13** gives intense $[P-30]^+$ ion (m/z 234), whereas this ion is not produced from MH^+ of **14**. The high energy CAD-MS/MS spectra of those ions at m/z 264 were, however, identical. The spectrum of $[MH-46]^+$ ion (m/z 263) gives $[P-30]^+$ ion which is scarcely formed from M^+ ion of **14**. These results indicate that the B/E constant linked scanning spectra of $[MH-45]^+$ and $[MH-46]^+$ ions overlap each other. The B/E constant linked scan spectrum of MH^+ ion of **13** exhibits three intense peaks of $[MH-46]^+$, $[MH-75]^+$ and $[MH-89]^+$ ions (m/z 263, 234 and 220, respectively). These results were similar to those obtained from the pair of **1** and **8**. The FAB spectra of **13** and **14**, the B/E constant linked scan spectra of $[MH-45]^+$ ion of **13** and MH^+ of

Fig. 8. FAB High Energy CAD-MS/MS Daughter Ion Spectra of the Ions of **13** and **14** at m/z 264 and 263

A1 and A2: $[MH-45]^+$ and $[MH-46]^+$ ions of **13**. B1 and B2: MH^+ and M^+ ions of **14**.

14, and the high energy CAD-MS/MS spectra of those ions are shown in Figs. 6, 7 and 8, respectively. The fragment ions of **13** are also shown in Chart 1.

Conclusion

FAB (LSIMS) spectra of β -blockers (nitrate ester) which have both a 3-amino-2-hydroxypropyl aryl ether moiety and a nitrate ester moiety exhibit intense $[\text{MH}-45]^+$ ions whose mass numbers are the same as those of the MH^+ ions of the corresponding hydrolysis products. Although the low energy CAD-MS/MS spectrum of $[\text{MH}-45]^+$ ion of the nitrate ester is identical with that of MH^+ of the hydrolysis product, the B/E constant linked scan spectra of $[\text{MH}-45]^+$ ions of the nitrate esters are different from the MH^+ ions of the hydrolysis products. To clarify the reason the two methods used for same purpose gave different results, high energy FAB CAD-MS/MS measurements were carried out. The CAD-MS/MS spectrum of $[\text{MH}-45]^+$ ions of the nitrate ester is identical with that of MH^+ ions of the hydrolysis product, but those of $[\text{MH}-46]^+$ and $[\text{MH}-47]^+$ ions of the ester are different from those of M^+ and $[\text{M}-1]^+$ ions of the hydrolysis product, respectively. A comparison between the results of B/E constant linked scanning and those of the high energy CAD-MS/MS indicates that the discrepancy is due to the poor resolutions of precursor ions in the B/E constant linked scanning and, as a result, the linked scan spectra of $[\text{MH}-45]^+$, $[\text{MH}-46]^+$ and $[\text{MH}-47]^+$ ions overlap one another. Low energy CAD-MS/MS mainly gives the daughter ions produced by cleavage in the amino alcohol moiety and gives few ions produced by cleavage of the skeleton part, whereas high energy CAD-MS/MS gives the daughter ions derived from both parts. This difference was

thought to be due to that in the CAD energy between quadrupole-type and sector-type instruments. Decomposition products of nipradilol by bombarding with the xenon beam (FAB) were also examined by HPLC and turned out to be different from those obtained by heating in glycerol. The formation of the corresponding hydrolysis products under FAB conditions was confirmed by HPLC. In summary, we found 1) the first example of hydrolysis taking place under FAB (LSIMS) conditions, and 2) an unusual example of the reaction caused by FAB being different from that by heating.

Acknowledgement This work was partially supported by a Grant-in Aid for Scientific Research from the Ministry of Education, Science and Culture (NO. 60430007) of Japan.

References

- 1) M. Shiratsuchi, K. Kawamura, T. Akashi, M. Fujii and H. Ishihama, *Chem. Pharm. Bull.*, **35**, 632 (1987).
- 2) Y. Uchida, *Jpn. Heart J.*, **23**, 981 (1982); Y. Uchida, M. Nakamura, S. Suzuki, Y. Shirasawa and M. Fujii, *Arch. Int. Pharmacodyn. Ther.*, **262**, 132 (1983).
- 3) M. Yoneda, K. Tsujimoto, M. Ohashi, M. Shiratsuchi and Y. Ohkawa, *Org. Mass Spectrom.*, **25**, 146 (1990).
- 4) T. Nakamura, H. Nagaki and T. Kinoshita, *Mass Spectrosc.*, **36**, 81 (1988).
- 5) S. Gaskell (ed.), "Mass Spectrometry in Biomedical Research," John Wiley & Sons, Chichester, 1986, p. 141.
- 6) L. D. Detter, O. W. Hand, R. G. Cooks and R. A. Walton, *Mass Spectrom. Rev.*, **7**, 465 (1988).
- 7) J. Adams, *Mass Spectrom. Rev.*, **9**, 141 (1990); F. W. McLafferty (ed.), "Tandem Mass Spectrometry," John Wiley & Sons, New York, 1983, Chap. 6 and 7.
- 8) J. Adams and M. L. Gross, *J. Am. Chem. Soc.*, **108**, 6915 (1986); M. L. Gross, *Mass Spectrom. Rev.*, **8**, 165 (1989).
- 9) H. Budzikiewics and L. Grotjahn, *Tetrahedron*, **28**, 1899 (1972).